Electronic Supplementary Material (ESI) for RSC Advances.

Supplementary information

Efficient Photoluminescent Complexes from Visible and NIR Emitting Lanthanide containing Organic Sensitizers for Optoelectronic Devices

Zubair Ahmed and K. Iftikhar*

Department of Chemistry
Jamia Millia Islamia, New Delhi-110 025 (INDIA)
Email: kiftikhar@jmi.ac.in
Phone: +91-11-26837297, Fax: +91-11-26980229/26982489

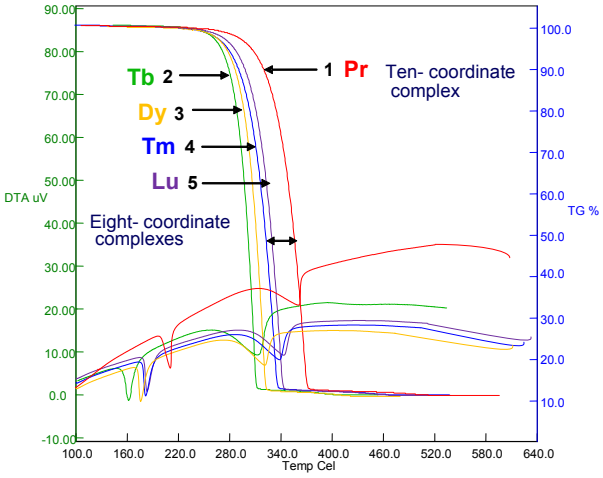

Fig.S1.TG/DAT plots of (**1**)[Pr(hfaa)$_3$(bpy)$_2$], (**2**) [Tb(hfaa)$_3$(bpy)$_2$], (**3**)[Dy(hfaa)$_3$(bpy)], (**4**) [Tm(hfaa)$_3$(bpy)] and (**5**)[Lu(hfaa)$_3$(bpy)]

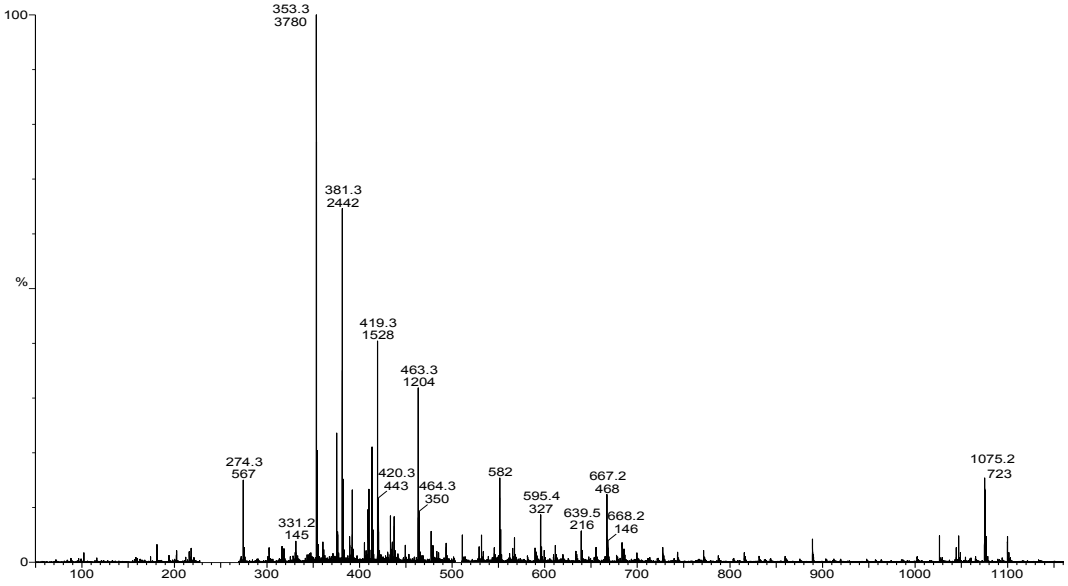

Fig. S2. Electrospray mass (ESI-MS$^+$) spectrum of [Pr(hfaa)$_3$(bpy)$_2$] in chloroform.

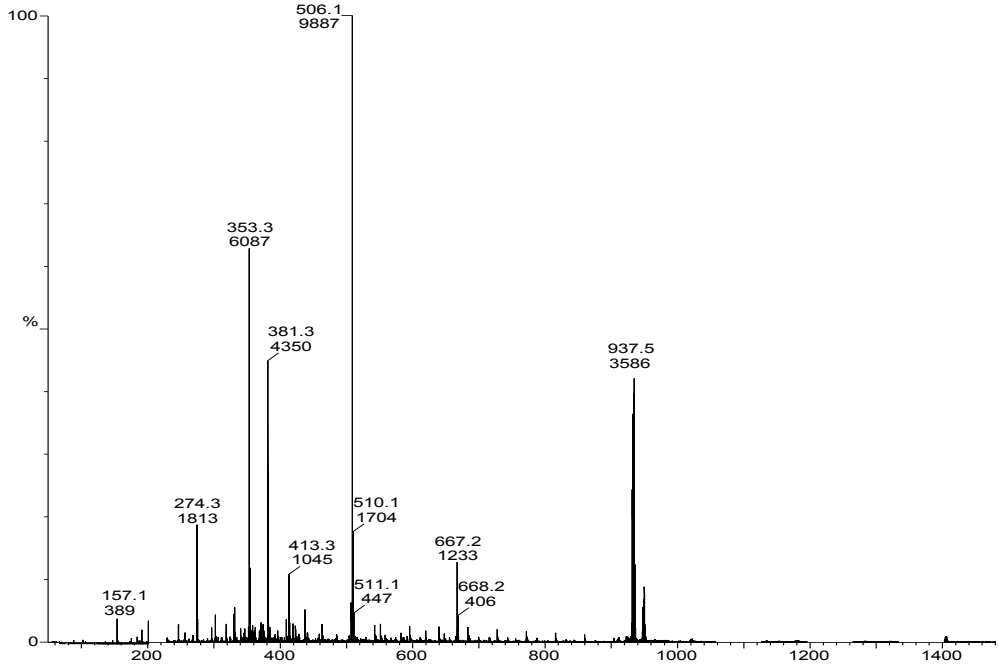

Fig. S3. Electrospray mass (ESI-MS$^+$) spectrum of [Tb(hfaa)$_3$(bpy)] in chloroform.

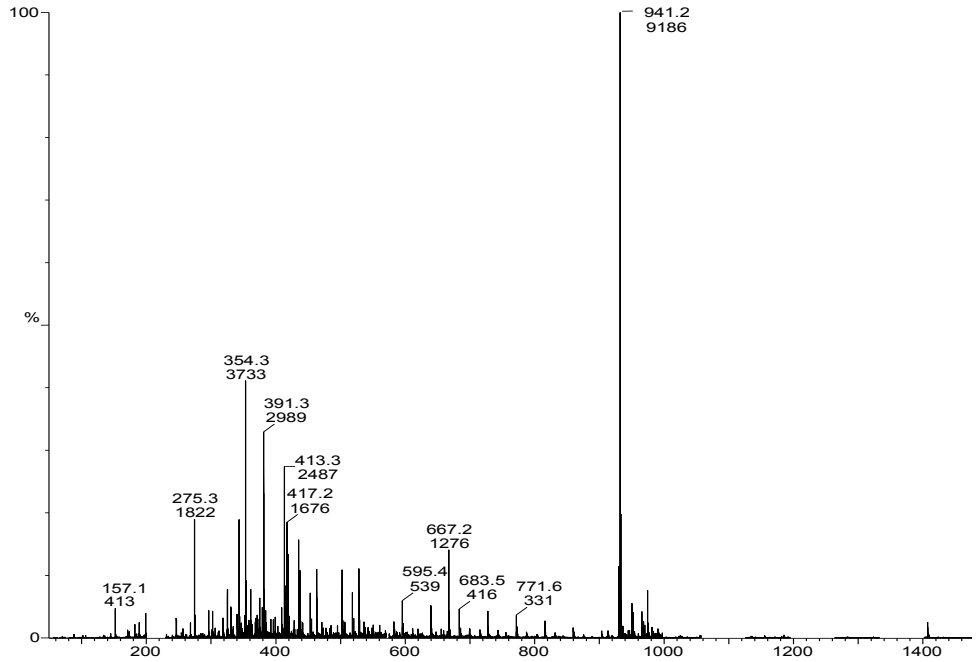

Fig. S4. Electrospray mass (ESI-MS$^+$) spectrum of [Dy(hfaa)$_3$(bpy)] in chloroform.

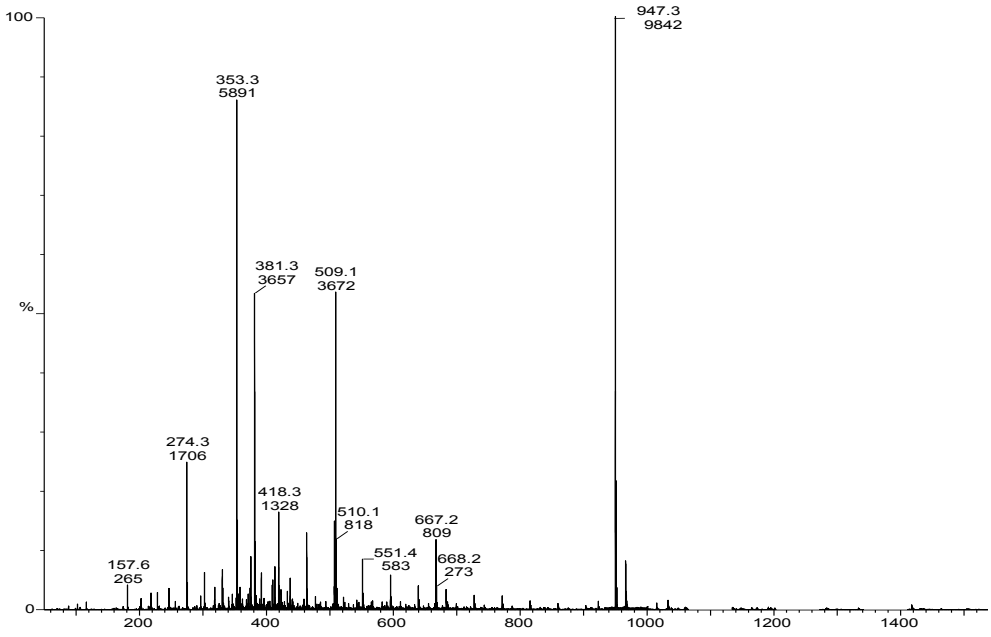

Fig. S5. Electrospray mass (ESI-MS$^+$) spectrum of [Tm(hfaa)$_3$(bpy)] in chloroform.

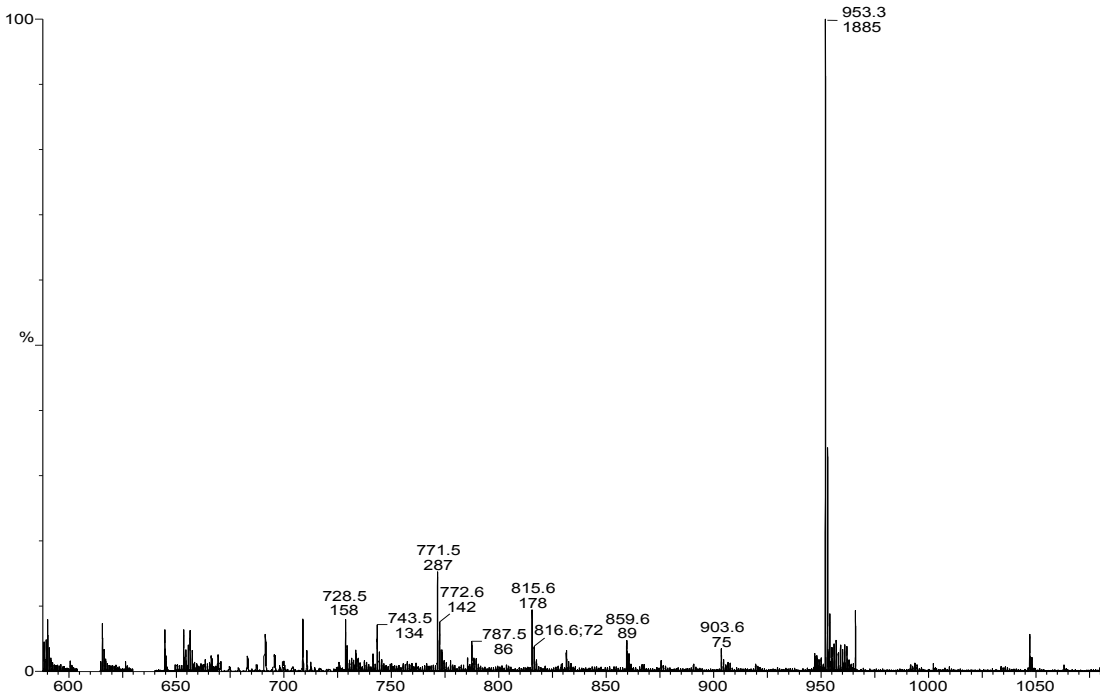

Fig. S6. Electrospray mass (ESI-MS$^+$) spectrum of [Lu(hfaa)$_3$(bpy)] in chloroform.

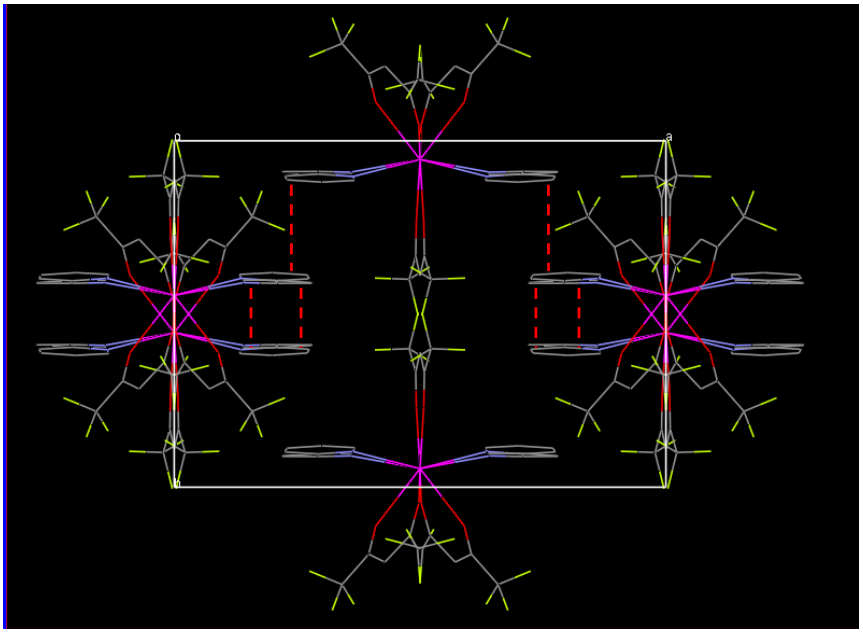

Fig. S7. Molecular packing of Pr complex, showing π−π stacking between the bpy units.

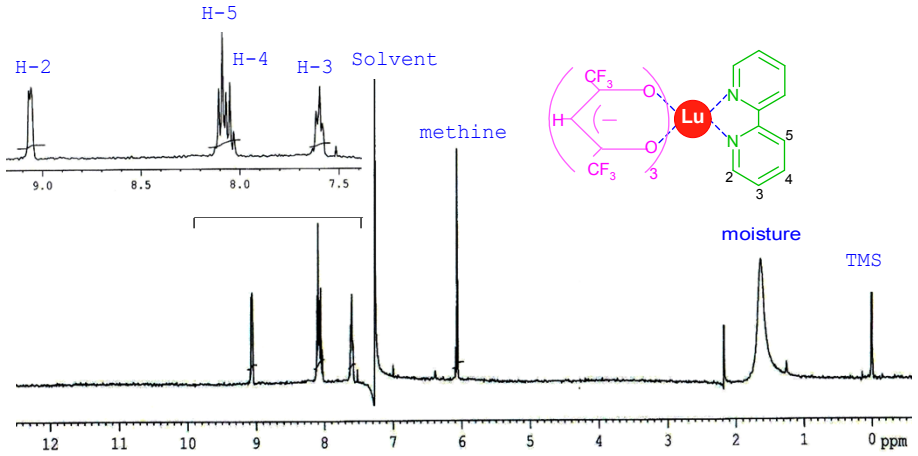

Fig. S8. ^{1}H NMR spectrum of $[Lu(hfaa)_3(bpy)]$ in $CDCl_3$. Inset showing the resolution of region from 7.5 to 9.5 ppm(δ).

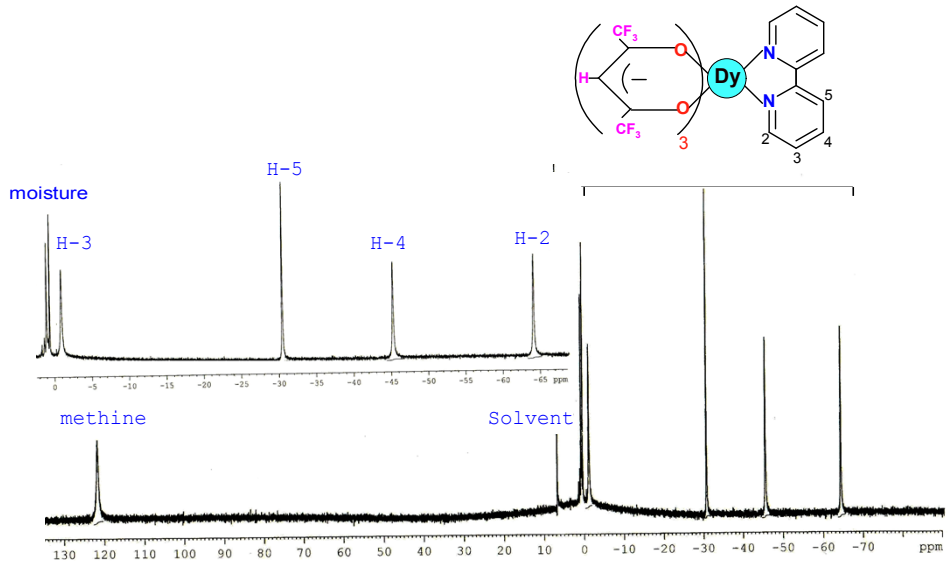

Fig. 9. ^{1}H NMR spectrum of $[Dy(hfaa)_3(bpy)]$ in $CDCl_3$. Inset: resolution of region from –65.0 to 0.0 ppm(δ).

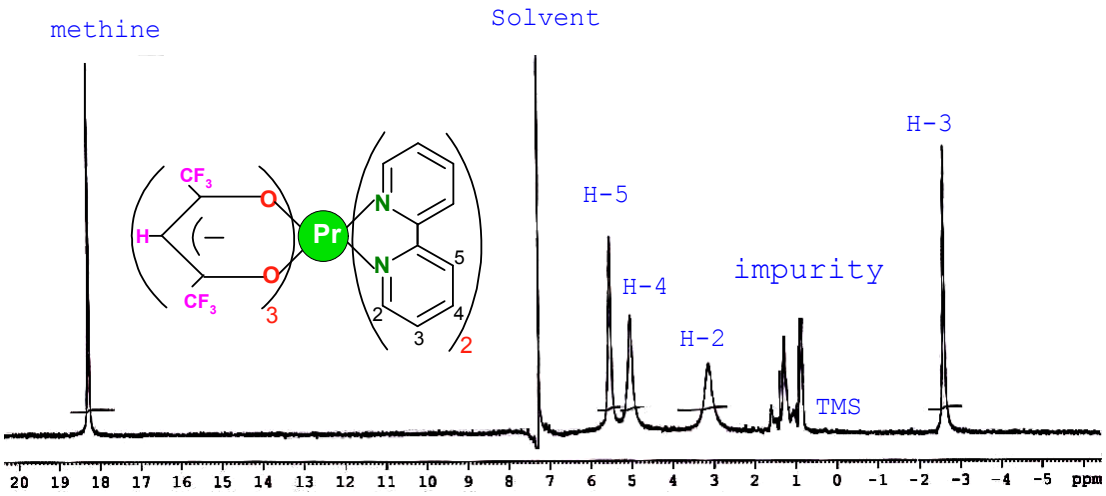

Fig. S10. ^{1}H NMR spectrum of [Pr(hfaa)$_3$(bpy)$_2$] in $CDCl_3$.

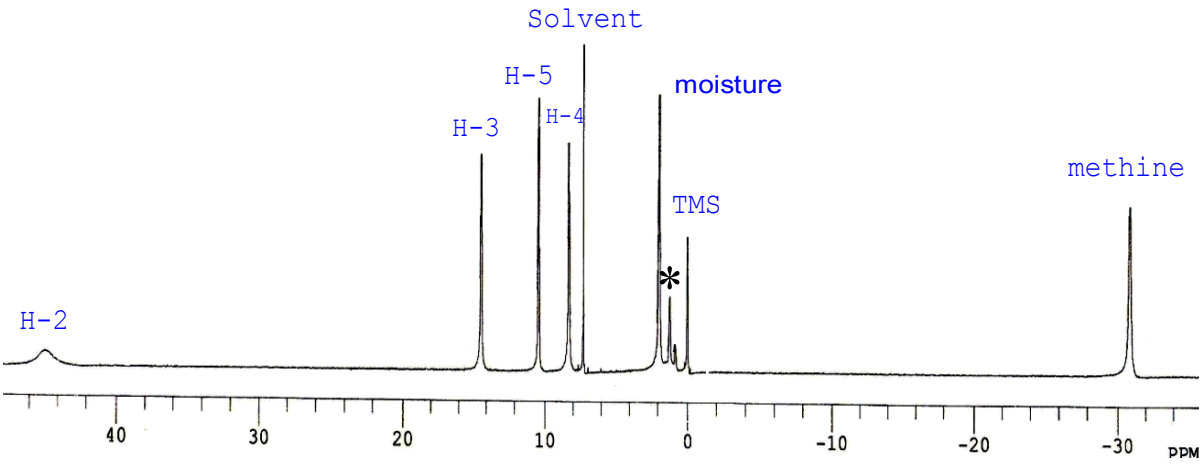

Fig. S11. ^{1}H NMR spectrum of [Tm(hfaa)$_3$(bpy)] in $CDCl_3$.*impurity.

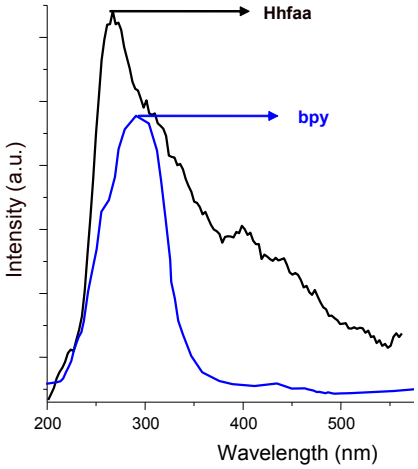

Fig. S12. Absorption spectra of Hhfaa and bpy in chloroform. (Concentration = 5×10^{-5} M).

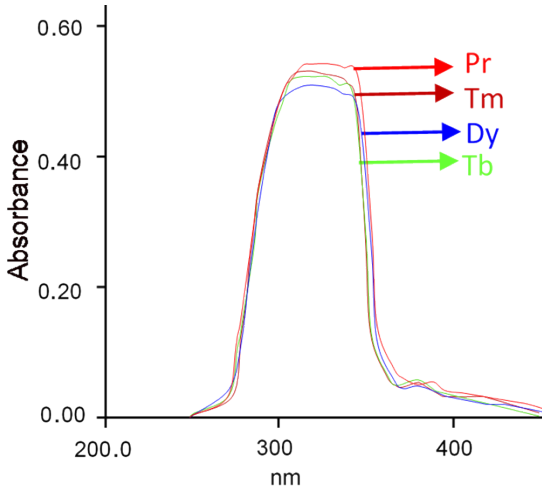

Fig. S13. Absorption spectra of [Pr(hfaa)$_3$(bpy)$_2$](λ_{max}= 321 nm), [Tb(hfaa)$_3$(bpy)] (λ_{max}= 322 nm), [Dy(hfaa)$_3$(bpy)$_2$] (λ_{max}= 320 nm) and [Tm(hfaa)$_3$(bpy)] (λ_{max}= 318 nm) in chloroform (Concentration = 5×10^{-5} M).

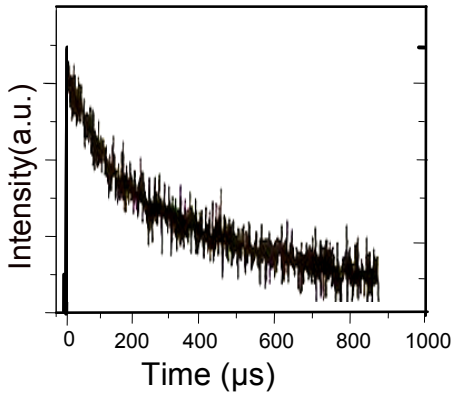

Fig. S14. Emission decay curve of the Tb complex at 77 K.

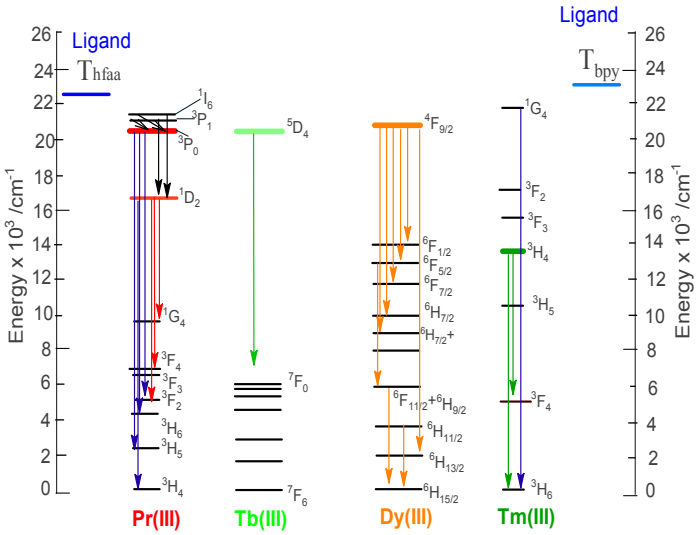

Fig. S15. The energy diagram showing lanthanide excited states and their position with respect to the triplet states of hfaa and bpy sensitizers.

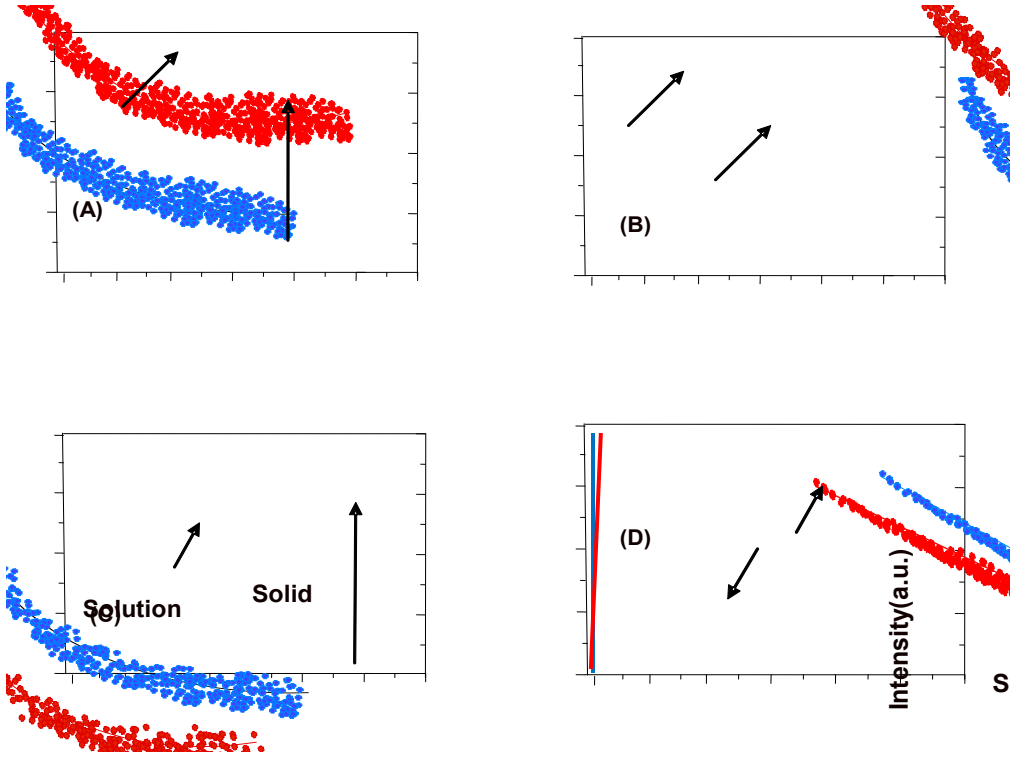

Fig. S16. Emission decay curve of the complexes, in visible region, in solution (blue) and solid state (red): Pr **(A),** Dy **(B)**, Tm **(C)** and Tb **(D).**

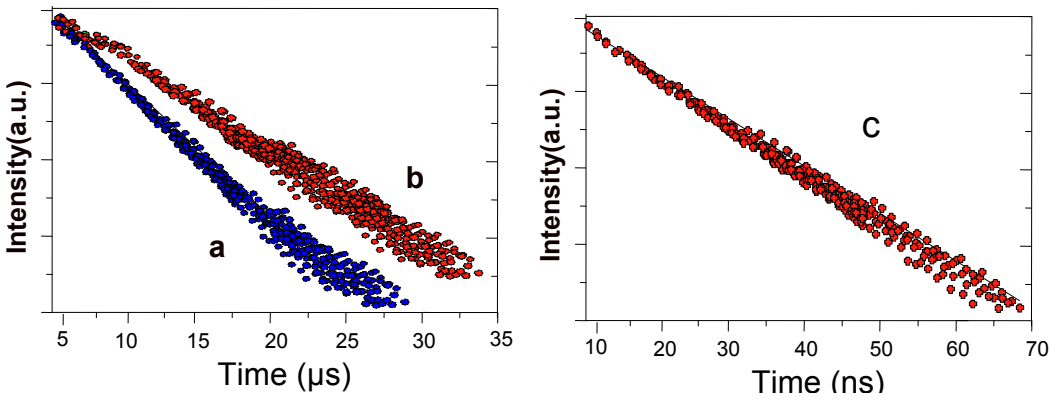

Fig. S17. Emission decay curve of the complexes in solution in NIR region: Pr **(a),** Dy **(b)** and Tm **(c).**

Table S1. Selected bond angles for the Pr complex.

O(2)-Pr(1)-O(2)#1	123.13(16)	O(3)-Pr(1)-(1)#1	132.17(13)	N(1)#1-Pr(1)-N(2)	117.33(14)
O(2)-Pr(1)-O(3)	68.23(12)	O(3)#1-Pr(1)-N(1)#1	70.46(13)	N(1)-Pr(1)-N(2)	58.22(15)
O(2)#1-Pr(1)-O(3)	67.51(12)	O(1)-Pr(1)-N(1)#1	65.66(12)	O(2)-Pr(1)-N(2)#1	71.26(15)
O(2)-Pr(1)-O(3)#1	67.51(12)	O(1)#1-Pr(1)-N(1)#1	93.30(13)	O(2)#1-Pr(1)-N(2)#1	118.19(15)
O(2)#1-Pr(1)-O(3)#1	68.23(12)	O(2)-Pr(1)-N(1)	69.21(14)	O(3)-Pr(1)-N(2)#1	131.73(14)
O(3)-Pr(1)-O(3)#1	75.41(18)	O(2)#1-Pr(1)-N(1)	123.89(14)	O(3)#1-Pr(1)-N(2)#1	65.51(13)
O(2)-Pr(1)-O(1)	151.66(12)	O(3)-Pr(1)-N(1)	70.46(13)	O(1)-Pr(1)-N(2)#1	99.76(14)
O(2)#1-Pr(1)-O(1)	85.02(11)	O(3)#1-Pr(1)-N(1)	132.17(13)	O(1)#1-Pr(1)-N(2)#1	64.29(13)
O(3)-Pr(1)-O(1)	128.18(12)	O(1)-Pr(1)-N(1)	93.30(13)	N(1)#1-Pr(1)-N(2)#1	58.22(15)
O(3)#1-Pr(1)-O(1)	134.42(12)	O(1)#1-Pr(1)-N(1)	65.66(12)	N(1)-Pr(1)-N(2)#1	117.33(14)
O(2)-Pr(1)-O(1)#1	85.02(11)	N(1)#1-Pr(1)-N(1)	155.42(19)	N(2)-Pr(1)-N(2)#1	161.7(2)
O(2)#1-Pr(1)-O(1)#1	151.66(12)	O(2)-Pr(1)-N(2)	118.19(15)		
O(3)-Pr(1)-O(1)#1	134.42(12)	O(2)#1-Pr(1)-N(2)	71.26(15)		
O(3)#1-Pr(1)-O(1)#1	128.18(12)	O(3)-Pr(1)-N(2)	65.51(13)		
O(1)-Pr(1)-O(1)#1	67.18(15)	O(3)#1-Pr(1)-N(2)	131.73(14)		
O(2)-Pr(1)-N(1)#1	123.89(14)	O(1)-Pr(1)-N(2)	64.29(13)		
O(2)#1-Pr(1)-N(1)#1	69.21(14)	O(1)#1-Pr(1)-N(2)	99.76(14)		

Table S2. Selected bond angles for the Dy complex.

Unit 1				**Unit 2**			
O5-Dy1-O6	73.00(14)	O5-Dy1-O1	148.73(14)	O10-Dy2-O11	75.44(15)	O10-Dy2-O9	75.34(14)
O5-Dy1-O3	74.10(14)	O6-Dy1-O1	81.02(15)	O10-Dy2-O12	117.29(15)	O11-Dy2-O9	137.27(16)
O6-Dy1-O3	136.60(14)	O3-Dy1-O1	117.01(14)	O11-Dy2-O12	72.39(13)	O12-Dy2-O9	149.88(14)
O5-Dy1-O4	81.33(15)	O3-Dy1-O1	75.61(14)	O10-Dy2-O7	137.26(14)	O7-Dy2-O9	72.77(13)
O6-Dy1-O4	75.85(15)	O2-Dy1-O1	71.31(14)	O11-Dy2-O7	146.00(14)	O8-Dy2-O9	79.47(15)
O3-Dy1-O4	71.88(14)	O5-Dy1-N2	75.67(16)	O12-Dy2-O7	81.26(15)	O10-Dy2-N4	143.75(15)
O5-Dy1-O2	138.92(16)	O6-Dy1-N2	114.57(16)	O10-Dy2-O8	72.45(15)	O11-Dy2-N4	79.92(15)
O6-Dy1-O2	145.27(15)	O3-Dy1-N2	83.23(18)	O11-Dy2-O8	119.61(15)	O12-Dy2-N4	78.86(15)
O3-Dy1-O2	76.35(14)	O4-Dy1-N2	149.90(16)	O12-Dy2-O8	79.05(14)	O7-Dy2-N4	74.11(14)
O4-Dy1-O2	115.43(15)	O2-Dy1-N2	73.06(15)	O7-Dy2-O8	74.36(15)	O8-Dy2-N4	143.72(15)
O1-Dy1-N2	132.40(15)	O2-Dy1-N1	79.20(15)	O9-Dy2-N4	107.54(15)	O8-Dy2-N3	147.96(15)
O5-Dy1-N1	109.82(16)	O1-Dy1-N1	79.12(16)	O10-Dy2-N3	82.54(18)	O9-Dy2-N3	74.99(15)
O6-Dy1-N1	75.23(15)	N2-Dy1-N1	63.95(17)	O11-Dy2-N3	70.89(15)	N4-Dy2-N3	64.33(15)
O3-Dy1-N1	143.59(15)			O12-Dy2-N3	131.39(15)		
O4-Dy1-N1	144.01(16)			O7-Dy2-N3	115.01(16)		

Table. S3. Chemical shifts[a] and paramagnetic shifts (Δδ)[b] of the complexes.

Compound		H(2)	H(3)	H(4)	H(5)	CH
Bpy		8.70	7.22	7.80	8.53	----
$[Pr(hfaa)_3(bpy)_2]$	**1**	3.12(s) (–5.95)	–2.63(s) (–10.23)	5.02(s) (–2.78)	5.52(s) (–2.59)	18.27 (11.67)
$[Tb(hfaa)_3(bpy)]$	**2**	–238.62(b) (–247.07)	–38.22(s) (–45.82)	–5.08(s) (–13.14)	1.96(s) (–6.15)	107.05 (100.99)
$[Dy(hfaa)_3(bpy)]$	**3**	–63.87(s) (–72.94)	–0.69(s) (–8.29)	–45.01(s) (–53.07)	–30.22(s) (–38.33)	122.27 (116.21)
$[Tm(hfaa)_3(bpy)]$	**4**	44.90(b) (35.834)	14.43(s) (6.83)	8.31(s) (0.25)	10.42(s) (2.31)	–30.94 (–37.00)
$[Lu(hfaa)_3(bpy)]$	**5**	9.07(d)	7.60(d)	8.06(s)	8.11(d)	6.06

[a]Chemical shift are relative to internal Me_4Si and are expressed in ppm (δ). Positive shifts are downfield and negative shifts are upfield.

[b]The paramagnetic shift is the difference between the chemical shift of the nucleus in the paramagnetic complex and the corresponding shift in the diamagnetic complex.

The Paramagnetic shifts are relative to the diamagnetic lutetium (III) complex.

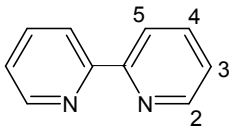

2, 2'-Bipyridine